

Slab-Phase Modulation Combined with Parallel Imaging in Bilateral Breast Imaging

M. Han^{1,2}, and B. A. Hargreaves¹

¹Radiology, Stanford University, Stanford, CA, United States, ²Electrical Engineering, Stanford University, Stanford, CA, United States

Introduction: Bilateral dynamic contrast enhanced (DCE) breast imaging requires high temporal and spatial resolution. Our protocol uses a dual-slab spectral-spatial pulse [1] to excite both volumes simultaneously and independently with excellent fat suppression. By incorporating slab-phase modulation within this pulse, the scan time can be reduced by not imaging the unexcited space between the volumes [2]. By exploiting the coil separation between the breasts, parallel imaging techniques can also increase acquisition speed. In this work, we will show the effects of phase modulation combined with self-calibrated parallel imaging using modified sensitivity encoding (mSENSE) [3] and generalized autocalibrating partially parallel acquisitions (GRAPPA) [4] on reconstructed image quality.

Materials and Methods: A phantom scan and six volunteer scans were conducted using a GE 1.5T Excite scanner and an eight-channel breast coil (GE Healthcare, Milwaukee, WI). For each scan, two experiments were performed using the dual-slab spectral-spatial pulse. The first experiment used phase encoding over the entire volume (both excited volumes and the space in between) with 192 sagittal 3D sections, 1.5 mm thick, and a 20 x 20 cm FOV. The second experiment used slab-phase modulation to virtually shift the slabs and phase encode only the two excited volumes [2], with 64 sagittal sections (1.5 mm thick) over each slab. A liquid phantom was scanned using a “stack-of-spirals” trajectory with 9 spiral interleaves, a 40° flip angle, 1.1 x 1.1 mm resolution and a 31 ms TR. The stack-of-spirals trajectory used phase-encoding in the left-right direction, so for this work can be treated similarly to a 3D Cartesian acquisition. Both sets of phantom experiments were repeated 22 times to measure SNR by the “multiple acquisition” method [5]. For the volunteer scans, a 3D Cartesian readout was used with a 30° flip angle, 512 x 128 matrix, and a 23 ms TR. Both sets of volunteer scans were repeated twice to measure SNR by the “difference method” [6].

To test parallel imaging, phase encode planes in the slice direction (k_z) were discarded to set the width of the acquired FOV as the thickness of one slab (Fig.1). For the data without slab-phase modulation, k_z planes were undersampled by a factor of three and slice-direction acceleration used mSENSE with a factor of two and GRAPPA with a factor of three. For the data with slab-phase modulation, k_z planes were undersampled by a factor of two and mSENSE and GRAPPA accelerations of two were used. An additional 20 planes were used for calibration, resulting in 31 central reference planes and 41 central reference planes without and with phase modulation, respectively. For the mSENSE reconstruction, low-resolution coil images from the hamming-windowed reference data were normalized by the square-root sum-of-squared magnitudes and used as sensitivity maps. For mSENSE without phase modulation, coil sensitivity maps were re-ordered according to actual slab overlap (See Fig 1). For the GRAPPA reconstruction, coil weight coefficients were estimated from the reference data. A paired student t-test was performed to compare SNR with and without phase modulation for both mSENSE and GRAPPA.

Results: Figure 2 shows axial reformatted images from the phantom without (a) and with (b) phase modulation. The first row shows the full k -space images, while the second and third rows show difference images between the mSENSE/GRAPPA reconstructions and the full k -space images averaged over the 22 acquisitions. Residual artifacts from the discontinuity of the mSENSE sensitivity maps and GRAPPA reconstruction errors shown by the arrows in (a) were not observed when phase modulation was used. Figure 2 (c) compares the mean SNR value of each method over the phantom, where the SNR was measured pixel-by-pixel from the 22 identical scans. The SNR improvement with phase modulation was measured in mSENSE to be 0.8 % and in GRAPPA to be 5 % with statistical significance ($p < 10^{-9}$). Figure 3 shows images from a single volunteer in the same manner as in Fig. 2. With phase modulation, fewer artifacts were observed. In (c), the mean SNR values were calculated from 30 ROIs located in the breast tissue of the six volunteers. With phase modulation, the mean SNR was higher in mSENSE by 7 % ($p = 0.0048$) and GRAPPA by 9 % ($p = 0.00003$).

Discussion: Slab-phase modulation with a dual-slab pulse reduces scan time in unaccelerated imaging, but also improves of image quality when self-calibrated parallel imaging is applied. For mSENSE, slab-phase modulation removes the need to re-order coil sensitivity maps and eliminates the artifacts from discontinuities in the sensitivity maps. For GRAPPA with slab-phase modulation, fewer additional calibration planes are required for estimation of coil weight coefficients, reducing the actual scan time. During *in vivo* imaging both GRAPPA methods yielded higher SNR than mSENSE, possibly because the imperfect sensitivity estimates lead to noise amplification in the mSENSE reconstruction. This is not the case in the phantom, where sensitivity values can be estimated more accurately.

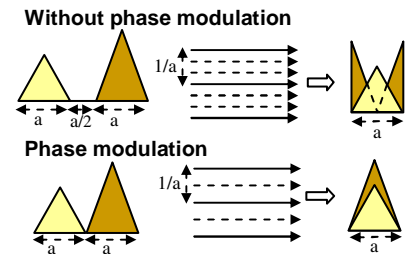


Figure 1. Undersampling without and with phase modulation. The data were undersampled to set the FOV as the thickness of one slab.

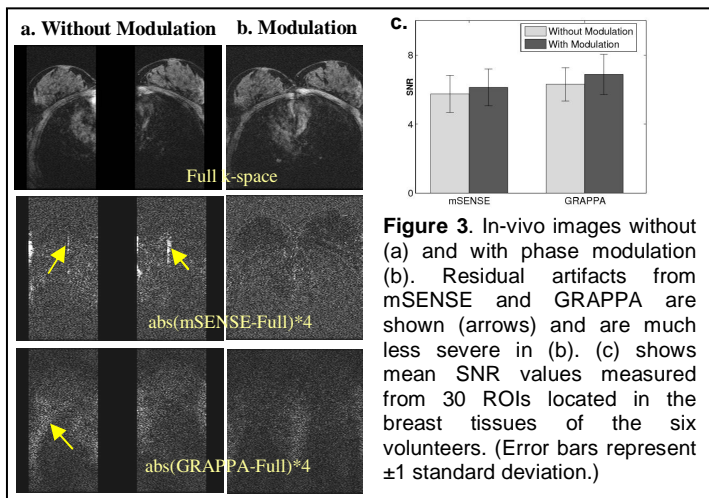


Figure 3. In-vivo images without (a) and with phase modulation (b). Residual artifacts from mSENSE and GRAPPA are shown (arrows) and are much less severe in (b). (c) shows mean SNR values measured from 30 ROIs located in the breast tissues of the six volunteers. (Error bars represent ± 1 standard deviation.)

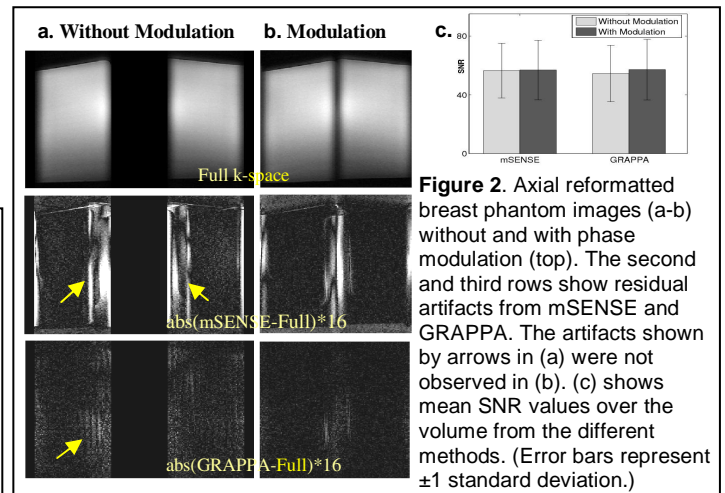


Figure 2. Axial reformatted breast phantom images (a-b) without and with phase modulation (top). The second and third rows show residual artifacts from mSENSE and GRAPPA. The artifacts shown by arrows in (a) were not observed in (b). (c) shows mean SNR values over the volume from the different methods. (Error bars represent ± 1 standard deviation.)

References

- [1] Pauly JM, et al., Proc., 11th ISMRM, p966, 2003.
- [2] Hargreaves BA, et al., Magn Reson Med, 57 (4):782-802, 2007.
- [3] Wang J, et al., Proc., 1st Wurzburg Workshop on Parallel Imaging, P92, 2001.
- [4] Griswold MA, et al., Magn Reson Med, 47, 1202-1210, 2002.
- [5] Reeder SB, et al., Magn Reson Med, 54, 748-756, 2005.
- [6] Firbank, et al., Phys Med Biol, 44, N261-N264, 1999.